Laplace-Gradient Wavelet Pyramid and Multiscale Tensor Structures Applied on High-Resolution DEMs

M. Kalbermatten[1], D. Van De Ville[2], S. Joost[1], M. Unser[2] , F. Golay[1]

[1] Ecole Polytechnique Fédérale de Lausanne (EPFL), GIS laboratory, Station 18, 1015 Lausanne, Switzerland
Telephone (+41) 21 693 57 83
Fax: (+41) 21 693 57 90
Email: {michael.kalbermatten, stephane.joost, francois.golay}@epfl.ch

[2] Ecole Polytechnique Fédérale de Lausanne (EPFL), Biomedical Imaging Group, Station 17, 1015 Lausanne, Switzerland
Telephone: (+41) 21 693 51 42
Fax: (+41) 21 693 37 01
Email: {dimitri.vandeville, michael.unser}@epfl.ch

1. Introduction

Wavelet decompositions are a powerful tool for multiscale image analysis. Their use in DEMs (Digital Elevation Models) analysis is still limited. Nevertheless, some researchers (De Boer 1992, Wilson & Gallant 2000) demonstrated that scale and structure play an important role to determine the elementary shape of landscape features. Wavelets are ideally localized functions fulfilling that condition (Mahler 2001, Gallant & Hutchinson 1996).

Wavelet analysis of high-resolution (1-meter) DEMs is highly complementary to morphometric indicators (Wood 1996); e.g., applications include multiscale filtering and enhancement. Here, we introduce various methods using wavelets and structure tensors in order to show the multiscale nesting of landscape features. The method was applied on a DEM including a well-known landslide, and the results were compared to an ordinary geomorphological analysis. The aim is to show the potential of this method and to give hints for further development of such tools in terrain analysis systems.

2. Methodology

2.1 Laplace-Gradient Wavelet Pyramid

Classical wavelet transforms (Mallat 1996, Mallat 2000) act like a smoothed multiscale derivative operator when applied to the data. Usually, multidimensional data is processed in a separable way, i.e. dimension-by-dimension, which leads to multiple wavelets at each scale making the interpretation difficult. The recently introduced “Marr wavelet pyramid” (Van De Ville et al. 2008b) is an intrinsic 2-D wavelet design inspired on David Marr’s theory of primate’s vision (Marr 1982) that circumvents these limitations. Each scale is characterized by a single wavelet that acts like a Laplace-complex gradient operator. Consequently, the wavelet coefficients are complex-valued and their phase provides directional information.

Marr’s theory proposes that vision (or human visual capabilities) is linked to information cells tuned into different spatial frequencies, thus making it possible to do multiscale analysis. For this purpose, wavelets are a useful tool for DEM analysis.

The starting point of the wavelet pyramid is the identification of the Laplace-complex gradient, which characterizes the complete family of shift-invariant, scale-invariant, and rotation-covariant convolution operators (Equation 1, Van De Ville & Unser 2008b).

$$L_{\gamma,N} = (-\Delta)^{\frac{\gamma-N}{2}} \left(-j\frac{\partial}{\partial x} - \frac{\partial}{\partial y} \right)^N \tag{1}$$

Next, the associated wavelet function is a multiscale version of this operator; i.e., the wavelet is defined as $\psi = L_{\gamma,N}(\phi)$, where ϕ is an appropriate smoothing kernel.

The scaling function associated with the wavelet pyramid is the so-called complex polyharmonic B-spline $\beta_{\gamma,N}$ in 2-D (Van De Ville et al. 2008b, Van De Ville et al. 2005); its scaling relation for dyadic subsampling (factor of 2 in each dimension) can be expressed conveniently in the Fourier domain by the low-pass filter H (Equation 2).

$$\hat{\beta}_{\gamma,N}(2\boldsymbol{\omega}) = \frac{1}{4} H(e^{j\boldsymbol{\omega}}) \hat{\beta}_{\gamma,N}(\boldsymbol{\omega}) \tag{2}$$

The wavelet function is embedded in the finer approximation scale; i.e., the high-pass filter W expresses the relationship in Equation 3.

$$\hat{\psi}_{\gamma,N}(2\boldsymbol{\omega}) = \frac{1}{4} W(e^{j\boldsymbol{\omega}}) \hat{\beta}_{\gamma,N}(\boldsymbol{\omega}) \tag{3}$$

Here, we use $\gamma = 3$ (number of vanishing moments) and $N = 1$ (order of the complex gradient). Consequently, the wavelet transform corresponds to a multiscale version of the operator $L_{3,1}$ (Equation 1).

To obtain the pyramid decomposition of the signal of interest, we apply the efficient filterbank algorithm depicted in Fig. 1. The decomposition is applied iteratively to the low-pass coefficients $c_{i-1}[\mathbf{k}]$. The wavelet coefficients are not subsampled, which leads to a pyramid structure with mild redundancy. In this paper, we chose up to eight decomposition levels.

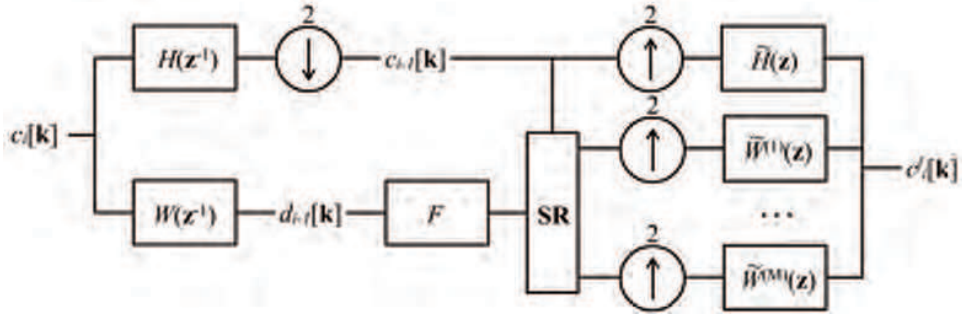

Figure 1. Laplace-gradient wavelet pyramid filterbank (adapted from Van De Ville et al. 2008b).

Before applying the synthesis procedure, we can process the wavelet coefficients ($d_{i-1}[\mathbf{k}]$), as embodied in the box F of Fig. 1. The synthesis procedure uses a so-called subband regression method to obtain the most consistent reconstruction with respect to the (redundant) decomposition (box **SR** in Fig. 1, see Unser & Van De Ville 2008 for more details).

2.2 Structure Tensors

Structures tensors are a representation of pixel value changes in a local neighbourhood. The complex-valued wavelet coefficients can be interpreted directly as the gradient of a Laplace-filtered and multiscale smoothed version of the data; i.e., we have $\nabla g_i[\mathbf{k}] = [\mathrm{Im}\{d_i[\mathbf{k}]\}, \mathrm{Re}\{d_i[\mathbf{k}]\}]$. Therefore, the wavelet coefficients can be used to compute a multiscale structure tensor (Van De Ville et al. 2008a):

$$\mathbf{J}_i(\mathbf{k}) = \sum_{\mathbf{n}\in\Omega} w[\mathbf{n}](\nabla g_i(\mathbf{k}+\mathbf{n})\nabla g_i(\mathbf{k}+\mathbf{n})^T) \quad (4)$$

where w is a fixed-size smoothing window with positive weights.

The eigenvectors and eigenvalues of the structure tensor provide robust and essential information about the signal variation at a given scale. Specifically, we did use the following three measures, obtained from the tensor (Van De Ville et al. 2008a):

- *Orientation*: orientation shows the dominant direction of the local structure. It is less prone to noise than the coefficient-wise orientation. Since the tensor is a second-order descriptor, there is no difference between a "positive" and a "negative" edge; i.e., gradients pointing in opposite directions are considered equally ($orientation \in [-\pi/2, \pi/2]$).
- *Energy*: energy of the the local gradient.
- *Coherency*: the ratio between the mean square magnitude of the gradient and the magnitude of the orientation vector gives an indicator called the coherency ($coherency \in [0,1]$). Large coherency shows that there is a dominant orientation in the local neighbourhood (depending on the Gaussian window's size) and small coherency indicates isotropy (Van De Ville et al. 2008a, Jähne 2005).

In order to have a comprehensive visualization of these measures, the 3 components are combined in a composite HSB (hue-saturation-brightness) image. The orientation was coded in the hue level (colour tint), the coherence in the saturation level and the energy in the brightness level. We applied histogram equalization to the energy component, since some initial adjacent pixels (elevations) have markedly different values. These ones induce much higher energy values than most of the other pixels. A root function (3rd or 4th order, depending on the decomposition level) was used to soften this effect.

Figure 2. Landslide context in Travers, Switzerland, DEM©SITN.

3. Application on High-Resolution DEMs

The proposed methodology was applied on a high resolution DEM (base resolution 1m) covering a recent landslide (2007) in Travers – Canton de Neuchâtel, Switzerland. The DEM was generated using TIN (Triangular Irregular Network) interpolation on raw scan2map[1] airborne LiDAR (Light Detection And Ranging) points. The resulting shaded DEM and the delimitation of the contained landslide are shown in Fig. 2.

3.1 Phase and Magnitude of the Complex Wavelet Subbands

The wavelet coefficients are complex-valued: phase (inverse tangent of the real and the imaginary parts) indicates the orientation and magnitude (squared root of the squared real and the squared imaginary parts) represents the strength. An example is shown in Fig. 3.

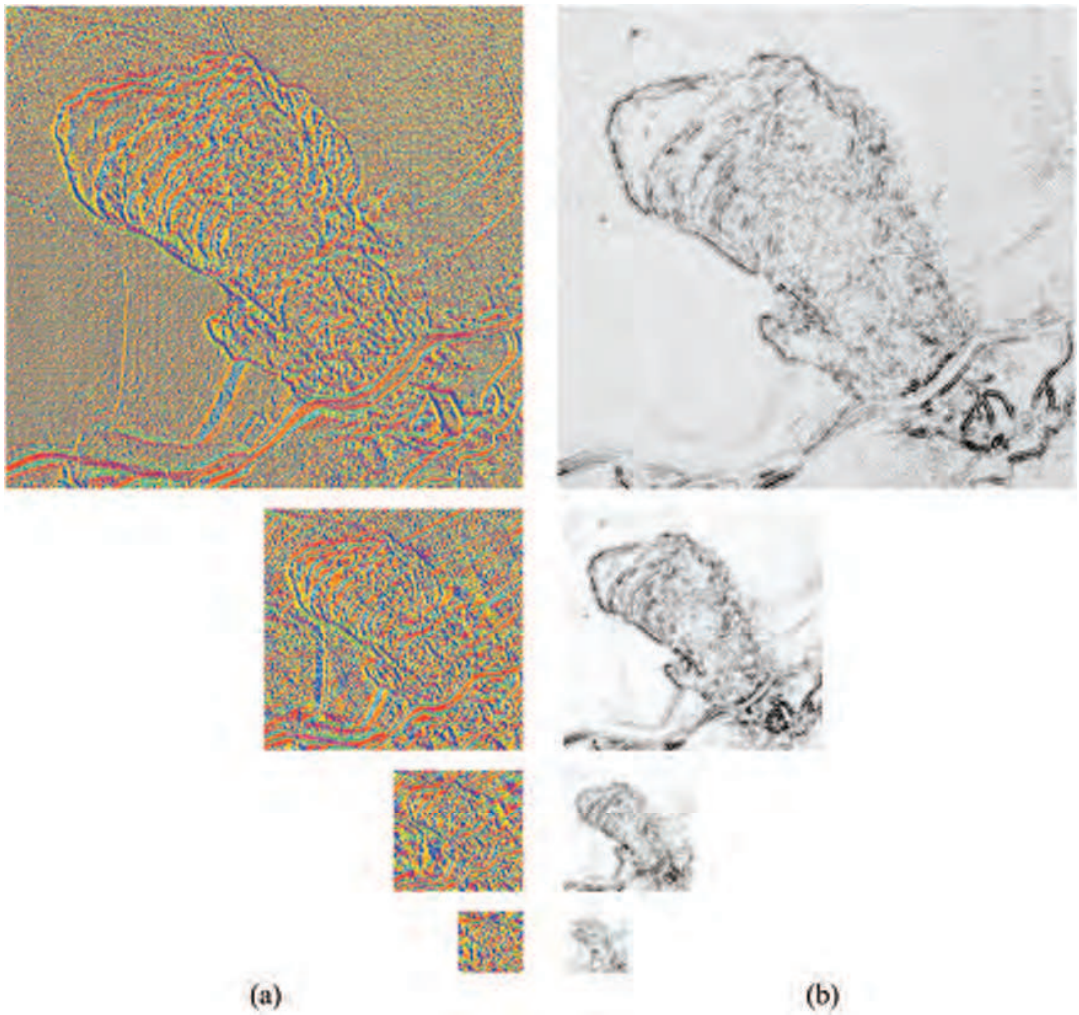

Figure 3. Phase (a) and magnitude (b) results on the landslide region for the first four decomposition levels (i.e. resolutions of 1, 2, 4 and 8 meters).

[1] scan2map is a research project of the Geodetic Engineering Laboratory at the Ecole Polytechnique Fédérale de Lausanne (TOPO-EPFL, see http://topo.epfl.ch/laserscanning/)

Phase and magnitude can also be combined to create a multiscale vector field. Each decomposition level shows the behaviour of its associated resolution. In Fig. 4, we show gradient vector fields using different decomposition levels.

We observe that the magnitude reveals interesting structural features depending on the decomposition level (thus the equivalent resolution of the feature shape) and phase the azimuth of the feature. Both of these indicators may be used for multiscale Canny edge detection, but this was not undertaken in this paper.

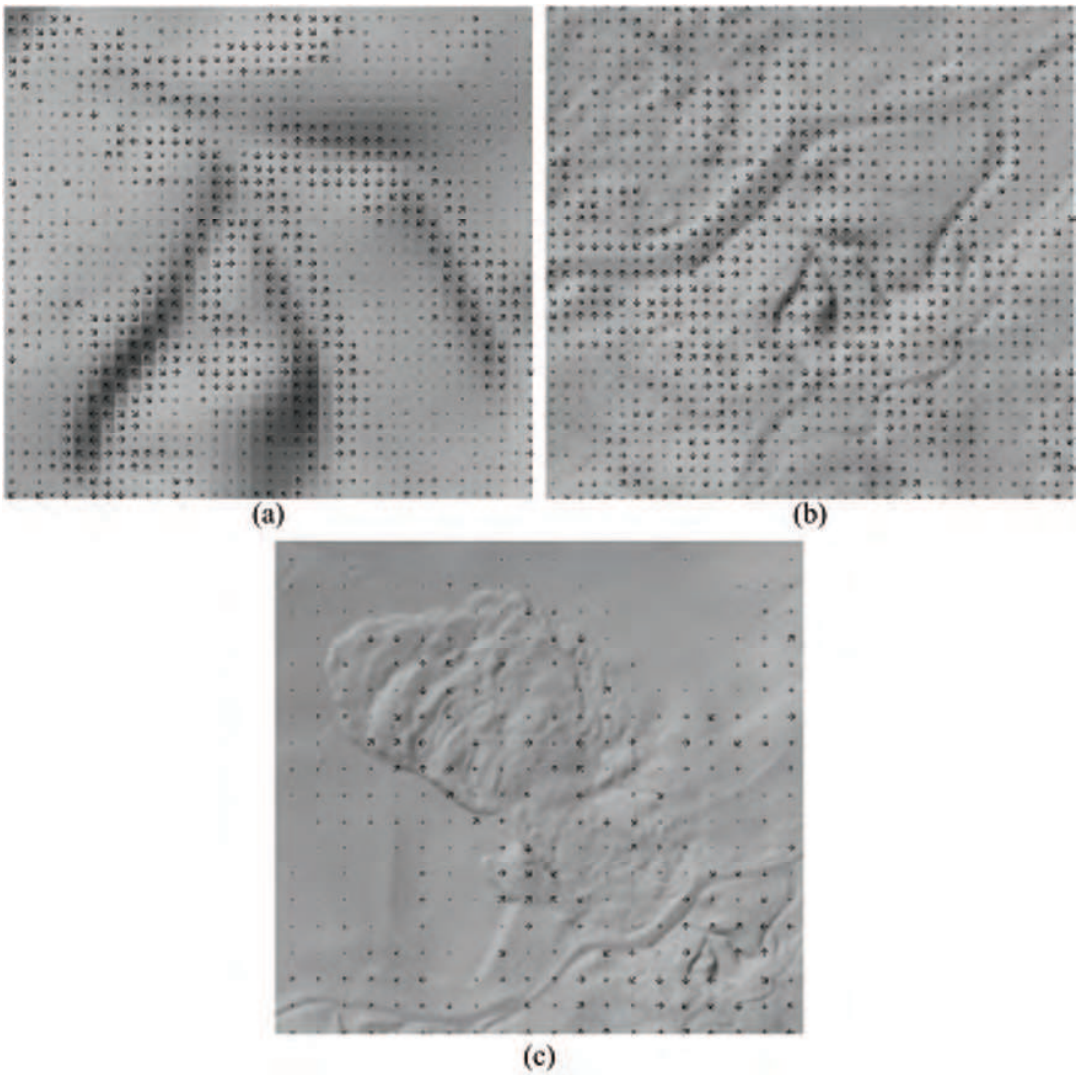

Figure 4. Phase-magnitude vector field for the first decomposition level (1m resolution) (a), for the third decomposition level (4m resolution) (b) and for the fifth decomposition level (16m resolution) (c).

3.2 Subband-selective Reconstruction

Reconstruction from specific subbands allows to choose which elements, based on their resolution (i.e. decomposition level), should be reconstructed to the finest scale (1 meter resolution). Fig. 5 shows the combination results of the different decomposition levels. The following procedure was used to create these images:

- The high resolution DEM was analysed until the n^{th} level.
- The resulting low pass grid was suppressed.
- The Marr pyramid was reconstructed using the subband regression.

The images in Fig. 5 are normalised ([-100,100]) coefficients with a colour saturation level at [-20,20]. Negative values are given in blue and positive values in red. The coefficients of the different levels were not enhanced (frequency boosting), but this could be done easily, depending on the interest of the geomorphologist.

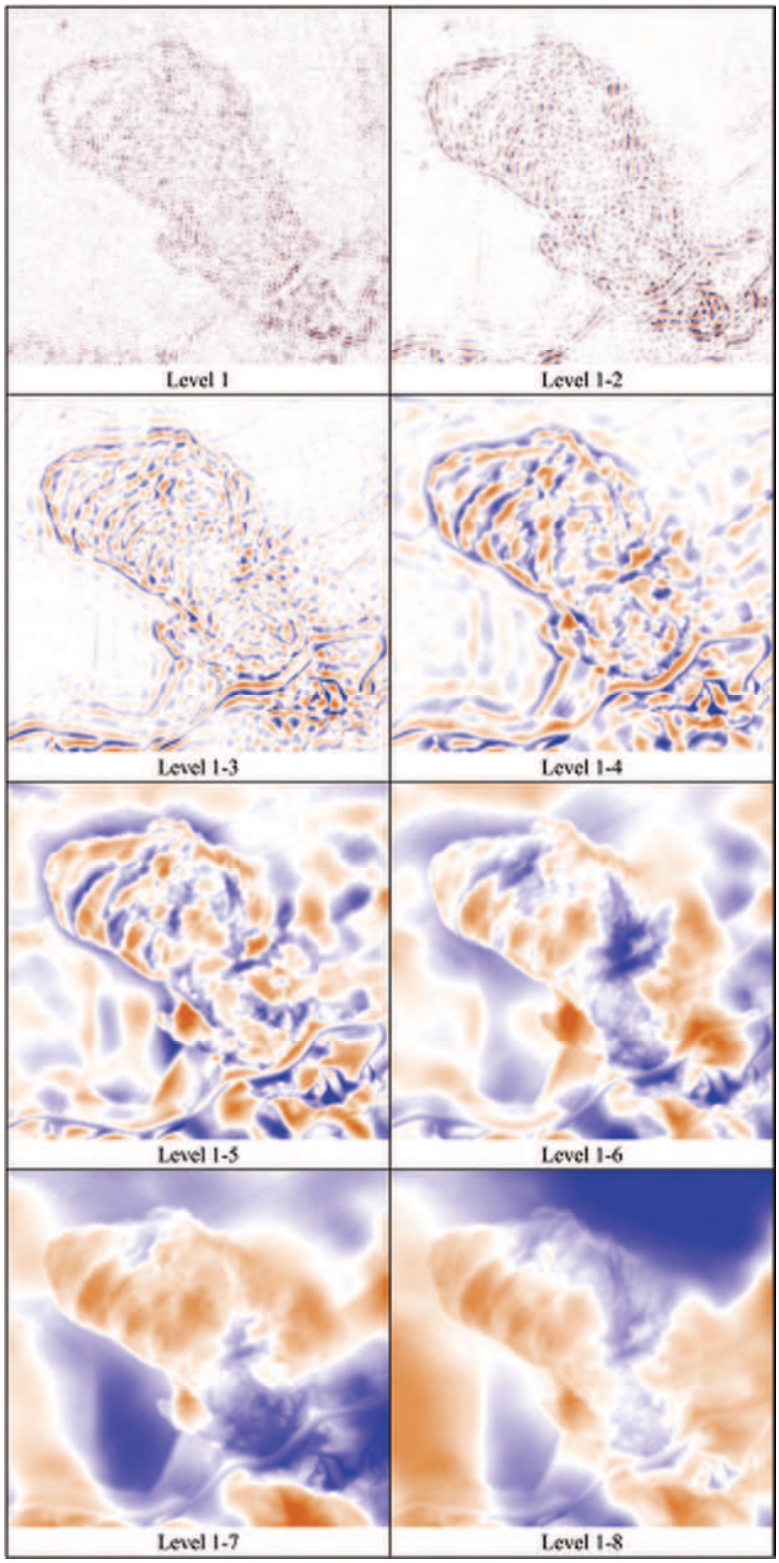

Figure 5. Subband reconstruction for cumulative high pass coefficients, from level 1 to cumulative level 1-8.

Fig. 5 illustrates the nesting of landscape structures and helps for the identification of pertinent morphological elements of the landslide. Any levels (filtered version or not) could be combined, to help multiscale feature recognition.

3.3 Structure Tensor of the Different Decomposition Levels

The different measures obtained from the multiscale structure tensor (coherency, energy and orientation) also provide excellent characterization of landscape elements. In Fig. 6, we show the results for the first decomposition level. As expected, coherency shows the isotropic behaviour of this level structures (whitest pixels) and energy (3rd root) the local energy of the coefficients. Fig. 6 was created using a 3x3 moving-average window.

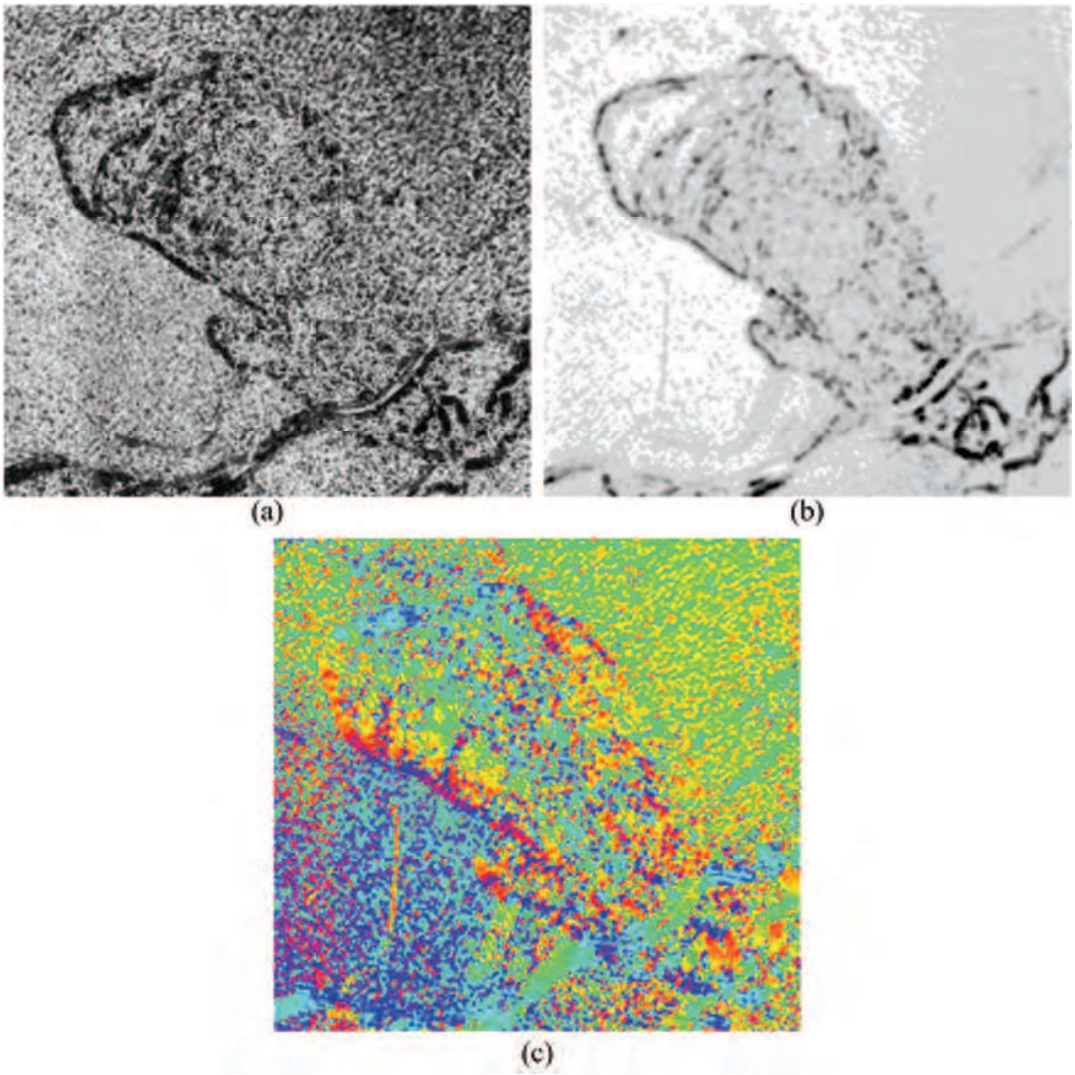

Figure 6. Structure tensor results for the first decomposition level, (a) coherency, (b) energy and (c) orientation.

Another representation of these results is given in Fig. 7 where the three new layers are coded in HSB image (H = orientation, S = coherency, B = energy). Going through the decomposition level, the images show more and more generalized structures.

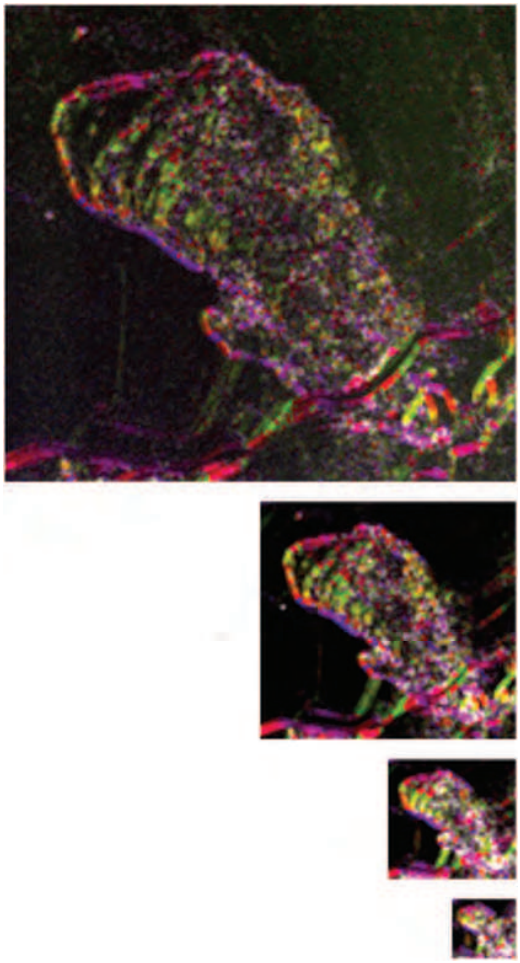

Figure 7. HSB images of structure tensor results for the first four decomposition levels.

4. Conclusion

We propose a novel DEM multiscale analysis approach. It is built upon recent advances in multidimensional wavelet design, in particular the Laplace-gradient wavelet pyramid. The phase and magnitude of the complex wavelet coefficients provide a unique representation of multiscale nested features. The combination of coefficients from distinct decomposition levels permits to obtain scale dependent structures corresponding to the needs of geomorphologists.

Localized and oriented multistructural information, as well as structure tensors, provide additional analytical elements. Combined to usual morphometry (Wood 1996), the proposed way of incorporating scale and structure may be useful to further elaborate landscape geomorphological processes.

References

De Boer D H, 1992, Hierarchies and spatial scale in process geomorphology: a review, *Geomorphology*, 4:303-318.

Gallant J C and Hutchinson M F, 1996, Towards an understanding of Landscape Scale and Structure, *Third International Conference/Workshop on Integrating GIS and Environmental Modeling*, Santa Fe, USA.

Jähne B, 2005, *Digital Image Processing, 6th revised and extended edition*, Springer, Berlin, Germany.

Mahler E, 2001, *Scale-Dependent Filtering of High Resolution Digital Terrain Models in the Wavelet Domain*, MSc Thesis, Department of Geography, University of Zurich, Switzerland

Mallat S, 1996, Wavelets for a vision, *Proceedings of the IEEE*, 84(4):604-614.

Mallat S, 2000, *Une exploration des signaux en ondelettes*, Les éditions de l'école polytechnique, France.

Marr D, 1982, *Vision: a computational investigation into the human representation and processing of visual information*, W. H. Freeman and Company, San Francisco, USA.

Unser M and Van De Ville D, 2008, The pairing of a wavelet basis with a mildly redundant analysis via subband regression, *IEEE Transactions on Image Processing*, 17(11):2040-2052.

Van De Ville D, Blu T and Unser M, 2005, Isotropic Polyharmonic B-splines: Scaling Functions and Wavelets, *IEEE Transactions on Image Processing*, 14(11):1798-1813.

Van De Ville D, Sage D, Balac D and Unser M, 2008a, The Marr wavelet pyramid and multiscale directional image analysis, *EUSIPCO08*, Lausanne, Switzerland.

Van De Ville D, and Unser M, 2008b, Complex wavelet bases, steerability, and the Marr-like pyramid, *IEEE Transactions on Image Processing*, 17(11):2063-2080.

Wilson J P and Gallant J C , 2000, *Terrain Analysis, Principles and Applications*, John Wiley & Sons, New-York, USA.

Wood J, 1996, *The Geomorphological Characterisation of Digital Elevation*, PhD Thesis, City university, London, UK.